Hindawi
Advances in Civil Engineering
Volume 2024, Article ID 5510839, 10 pages
https://doi.org/10.1155/2024/5510839

Research Article

Effects of Compaction Water Content on Water Retention and Deformation Behavior of Compacted Loess

S. J. Di,[1] Y. Zhang,[1] H. Zhou,[1] W. L. Xie,[2] X. L. He,[1] Y. T. Li,[1] and Q. Y. Mu[3]

[1]*Power China Northwest Engineering Corporation Limited, Xi'an, China*
[2]*State Key Laboratory of Continental Dynamics, Northwest University, Xi'an, China*
[3]*School of Geological Engineering and Geomatics, Chang'an University, Xi'an, China*

Correspondence should be addressed to Q. Y. Mu; 445953087@qq.com

Received 15 November 2023; Revised 21 December 2023; Accepted 28 December 2023; Published 19 January 2024

Academic Editor: Panpan Xu

Compacted loess is widely used as a construction material in engineering practices. The compaction dry density and compaction water content have significant effects on the hydromechanical behavior of compacted loess, thereby influencing the serviceability and safety of engineering structures. The former was widely studied in previous studies, while the latter is rarely known. In this study, the water retention, compression, and collapse behavior of compacted loess at different compaction water contents are investigated through pressure plate and oedometer tests. Microstructure analysis was carried out for insight analysis of the test results. The air entry value and yield stress of compacted loess decreased by 64% and 50%, respectively, with the compaction water content increasing from 12.4% to 19.0%. This is due to the fact that the number of clods increases with increasing the compaction water content, leading to many large-sized pores (i.e., diameter > 1,000 μm) and weaker soil skeletons. The influence of compaction water content on the water retention and compression behavior of loess is more pronounced at lower compaction dry densities and lower testing water contents, respectively. In addition, the specimen shows smaller collapse indexes at higher compaction water contents, mainly because of the larger deformation induced by the initial compression.

1. Introduction

In engineering practices, the compacted loess is widely used as the construction material, such as high-fills, embankments, and landfill covers [1–5]. As a typical structural soil, the deformation behavior of loess is significantly influenced by water content. During rainfall infiltration or groundwater fluctuation, compacted loess is subjected to wetting along the depth, leading to settlement and cracking of engineering structures [6, 7]. Therefore, it is significant to study the water retention and deformation behavior of compacted loess for addressing engineering issues in loess regions. Moreover, different compaction dry densities and compaction water contents result in various particle arrangements and pore structures of compacted soils [8–10], thereby affecting their water retention and deformation behavior. So far, numerous studies have been carried out on the water retention and deformation behavior of compacted soil [11–13]. However, researches on compacted loess have mainly focused on the influence of compaction dry density. The effects of compaction water content on the microstructure (e.g., particle arrangement and pore structure), water retention, and deformation behavior of compacted loess have been received relatively less attention.

The relationship between water content and suction is defined as the water retention curve (WRC), describing the water-holding capacity of unsaturated soil. Considerable progress has been made in the study of the WRC of compacted loess, and factors influencing the WRC of loess include dry density [14–16], temperature [9], wetting-drying cycles [17], and stress state [18]. Zhao and Wang [15] measured WRCs of compacted loess at different dry densities through pressure plate tests. Results showed that the water-holding capacity of loess increased with increasing dry density. Liu et al. [14] found that the effects of dry density on WRCs of compacted loess mainly appeared in air-entry value (AEV) and residual water content, with little influence on the desorption rate. Mu et al. [19] compared WRCs of natural loess and compacted loess with the same dry density and

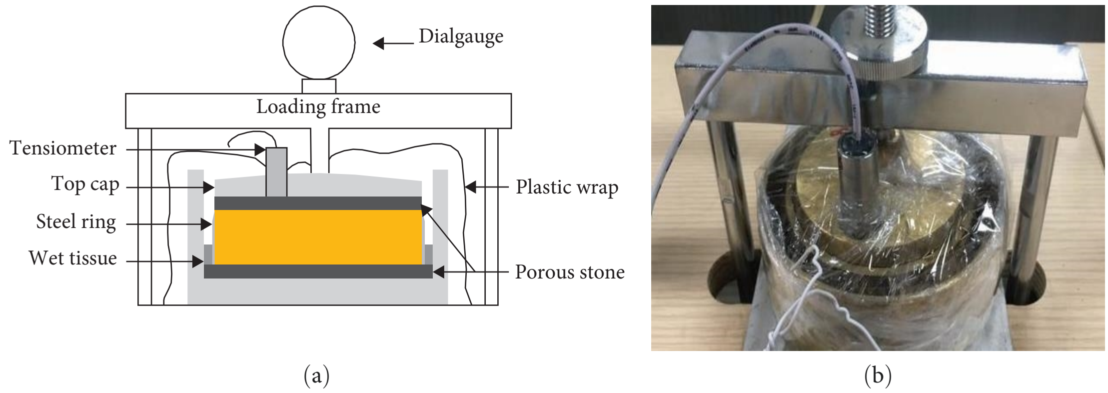

Figure 1: The modified oedometer apparatus: (a) schematic diagram; (b) photograph.

water content. Their results showed that the AEV of compacted loess was 75% higher than that of natural loess, and the hysteresis in WRC of natural loess varies slightly with wetting–drying cycles compared to compacted loess. Cheng et al. [9] studied the effects of temperature on WRCs of loess through triaxial tests. They found that the water-holding capacity of loess decreased with increasing temperature. Additionally, Wang et al. [20] concluded that the structural differences induced by different compaction water contents, which have significant effects on WRCs of loess. The water-holding capacity increases with the compaction water content increasing from the dry side of optimum water content to the optimum water content. The aforementioned study focused on the compaction water content range below the optimum water content, and there is a lack of research on the range of compaction water content exceeding the optimum water content.

As the deformation of loess reaches a stable state under a given stress, the additional deformation induced by an increase in water content is defined as wetting-induced deformation. The deformation that occurs when the loess is fully saturated is referred to as wetting-induced collapse. Previous studies investigated the wetting-induced deformation and collapse of compacted loess, mainly through 1D compression tests and isotropic compression tests. Huang et al. [21] found that the total deformation induced by compression and wetting of compacted loess decreases with increasing the dry density, while the proportion of wetting-induced deformation increases. Chen et al. [22] found that the structure changes caused by compaction water content have a significant influence on the compression behavior of loess at the same dry density and water content. Yang et al. [23] concluded that the initial water content, stress state, and dry density affect the wetting-induced collapse of loess to various extents. Wang et al. [24] found that under the same stress conditions, the wetting-induced collapse and peak collapse pressure of compacted loess increase with increasing suction. The above literature review further demonstrated that there have been more studies on the influence of compaction dry density on water retention and deformation behavior of loess, while literatures considering the effects of compaction water content are relatively scarce.

This study aims to investigate the effects of compaction water content on the water retention, compression, and collapse behavior of loess. To achieve this objective, a series of compacted specimens with different compaction water contents under given compaction densities are prepared. A commercial pressure plate is used to obtain WRCs, while the compression and collapse behavior are measured through a modified 1D compression apparatus with suction monitoring. In addition, microscopic analysis using a microscope is carried out to study the microstructure of compacted loess at different compaction water contents, which provides insightful explanations for the experimental results.

2. Experimental Apparatus

The WRCs were tested using the 1500F1 pressure plate apparatus from SoilMoisture Equipment Corp., USA. The equipment consists of three main components: an air pressure control device, a pressure chamber, and a suction and drainage measurement device. The pressure chamber uses an axial translation technique to control the soil suction. During the test, the specimen is placed on a saturated ceramic disk inside the pressure chamber (AEV: 5 bar), and the water reservoir beneath the ceramic disk is connected to the atmosphere through a plastic tube. By using the water reservoir beneath the ceramic disk as the reference plane, the pore water pressure (u_w) in the specimen is zero. Different suctions (u_a–u_w) are applied to the soil specimen by changing the air pressure (u_a) inside the pressure chamber. After reaching the equilibrium state, the soil specimen is removed from the pressure chamber and weighed to calculate the water content at each suction level. The suction equilibrium criterion is that the water content variation of the specimen within 24 hr is less than 0.04%. A more detailed description of the instrument is given by Mu et al. [17].

The compression and collapse behavior were measured using a modified oedometer. As shown in Figure 1, a hole was drilled in the top cap to install a tensiometer with a measurement range of 0–100 kPa. Prior to the test, the tensiometer was saturated using a chamber similar to that used in a previous study [25]. The suction variation of the soil specimen was measured during the compression and soaking

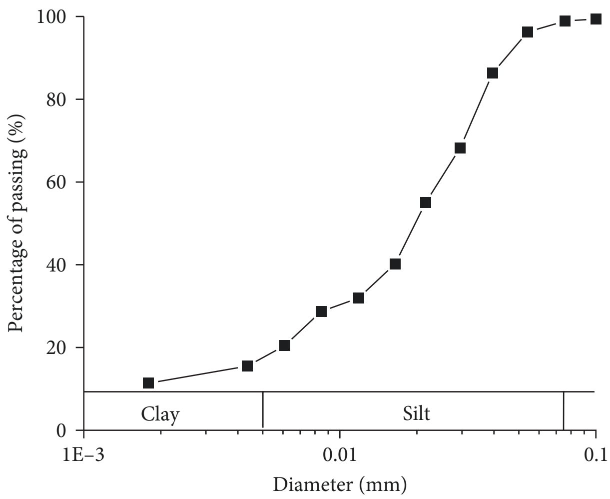

FIGURE 2: Particle size distribution of tested loess.

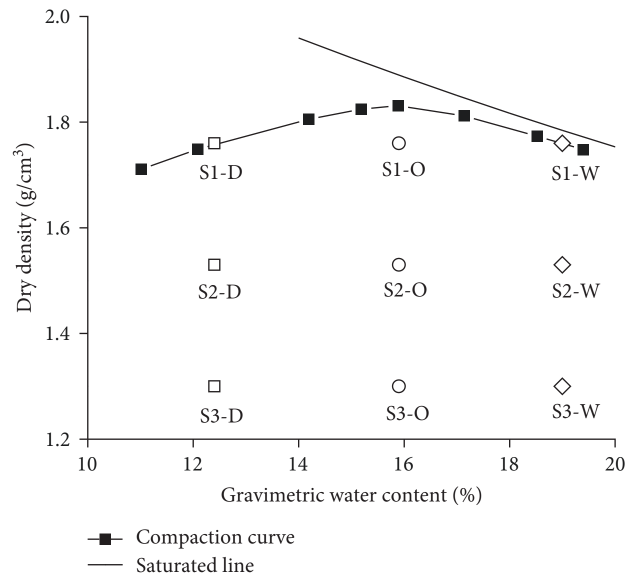

FIGURE 3: Compaction curve of tested loess.

stages. Since constant water content condition is required during the compression of the soil specimen, the consolidation cell was covered with cling film. Wet tissue was also filled around the oedometer ring to prevent moisture evaporation during the experiment.

In addition, the microstructure analysis was carried out using the Nikon SMZ1270 stereo microscope. This instrument allows for high-resolution image capturing and processing, which is used to analyze the arrangement of soil particles and pore structure.

3. Soil Property and Specimen Preparation

3.1. Soil Property. The loess used in this study was collected from a filling site in Yan'an, Shaanxi Province. According to the GB/T 50145 [26], the particle size distribution of the loess is measured and shown in Figure 2. The loess contains 17.4% clay-sized particles and 82.1% silt-sized particles. The plastic limit and liquid limit are 13.1% and 30.9%, respectively, according to ASTM [27] D4318-10. Based on the engineering classification for soil [26], the loess falls into the category of low-plasticity clay. The optimum water content and maximum dry density, which are obtained through laboratory proctor compaction tests [28], are 15.9% and 1.831 g/cm^3, respectively. In addition, the specific gravity of the tested loess is 2.67.

3.2. Specimen Preparation. The collected loess is first placed in an oven for drying. After drying, it is crushed and sieved through a 2-mm sieve. Water is sprayed onto the loess to achieve the predefined compaction water content. The loess is sealed in a plastic bag for 24 hr to ensure moisture equalization. The water content of the prepared loess is measured to ensure that the predefined compaction water content is reached with a deviation of less than 0.05%. For preparing soil specimens, the required mass of wet loess is calculated based on the predefined compaction dry density and compaction water content. The loess is uniformly compacted into an odeometer ring (i.e., 70 mm in diameter and 20 mm in height). The surface is then smoothed using a glass plate.

It should be noted that the compaction water content is different from the testing water content during the tests. When the compaction water content is lower than the testing water content, water is dripped onto the surface of the specimen using a dropper to increase the moisture content. For specimens with higher compaction water contents, the specimen is allowed to air-dry naturally to achieve the predefined testing water content. After the wetting or drying, the specimen is sealed in a plastic bag for moisture equalization. During this period, the suction is measured using a tensiometer to ensure that the suction is stabilized before carrying out tests.

4. Test Program

The compaction curve of the tested loess is shown in Figure 3. For the water retention tests, the dry densities of specimens are 1.30 g/cm^3 (S1), 1.53 g/cm^3 (S2), and 1.76 g/cm^3 (S3). The compaction water contents are 12.4% (W1, dry side of optimum water content), 15.9% (W2, optimum water content), and 19.0% (W3, wet side of optimum water content). A total of nine soil specimens were prepared. After preparation, the specimens were first saturated in the pressure chamber and suctions were applied to 400 kPa in steps.

For the compression tests, nine specimens were prepared at a compaction dry density of $\rho_d = 1.30$ g/cm^3 (S1) and compaction water contents of 12.4% (W1), 15.9% (W2), and 19.0% (W3). The specimens were then wetted or dried to testing water contents of 14.7% (W1), 17.4% (W2), and 19.8% (W3). During the compression tests, a loading frame was used to apply vertical loads up to 800 kPa using dead weights. A dial gauge was used to measure the vertical displacement of the soil specimens. The cutoff criterion for each loading step is that the deformation is less than 0.001 mm/hr (volumetric strain rate less than 0.005%/hr).

For the collapse tests, three specimens were prepared at a compaction dry density of 1.30 g/cm^3 (S1) and compaction

Table 1: Test programs of water retention, compression, and collapse tests.

Test no.	Dry density, ρ_d (g/cm^3)	Compaction water content, w (%)	Testing water content, w (%)
S1-D		12.4	
S1-O	1.30	15.9	19.6
S1-W		19.0	
S2-D		12.4	
S2-O	1.53	15.9	28.2
S2-W		19.0	
S3-D		12.4	
S3-O	1.76	15.9	39.7
S3-W		19.0	
S1-D-W1			14.7
S1-D-W2		12.4	17.4
S1-D-W3			39.7
S1-O-W1			14.7
S1-O-W2	1.30	15.9	17.4
S1-O-W3			39.7
S1-W-W1			14.7
S1-W-W2		19.0	17.4
S1-W-W3			39.7
S1-D-W1		12.4	
S1-O-W1	1.30	15.9	14.7
S1-W-W1		19.0	

(a) (b) (c)

Figure 4: Images of loess compacted at different water contents: (a) dry of optimum; (b) optimum; (c) wet of optimum.

water contents of 12.4% (W1), 15.9% (W2), and 19.0% (W3). The specimens were then subjected to wetting or air-drying to achieve a water content of 14.7% (W1). Similar to the compression tests, a loading frame was used to apply a vertical load of 200 kPa, followed by soaking through water immersion and then loading up to 800 kPa. The cutoff criteria for each loading step and soaking are also similar to that of compression tests (i.e., volumetric strain rate less than 0.005%/hr for at least 1 hr). More detailed test programs for the water retention, compression, and collapse tests are given in Table 1.

5. Result Interpretations

5.1. Microstructure Analysis. Figure 4 shows the microscopic images of the specimens at the compaction dry density of 1.30 g/cm^3 and different compaction water contents (i.e., dry side of the optimum water content, optimum water content, and wet side of the optimum water content). At the dry side of optimum water content, silt and clay particles form aggregates, with interaggregate pores between them. Moreover, previous studies showed that there were intra-aggregate pores between the silt/clay particles within the aggregates [8]. The aggregates and bi-modal pore size distribution were widely observed in previous studies on compacted silty and clayey soils [8, 10, 29, 30]. At the optimum water content and wet side of optimum water content, the images also show aggregates and bi-modal pore size distributions. Furthermore, the sizes of the aggregates and interaggregate pores gradually increase with an increase in the compaction water content. Particularly, many large aggregates (i.e., >1,000 μm) and interaggregate pores (i.e., >1,000 μm) are formed at the wet side of optimum water content. This is because a large number of clods are formed when the loess is mixed with

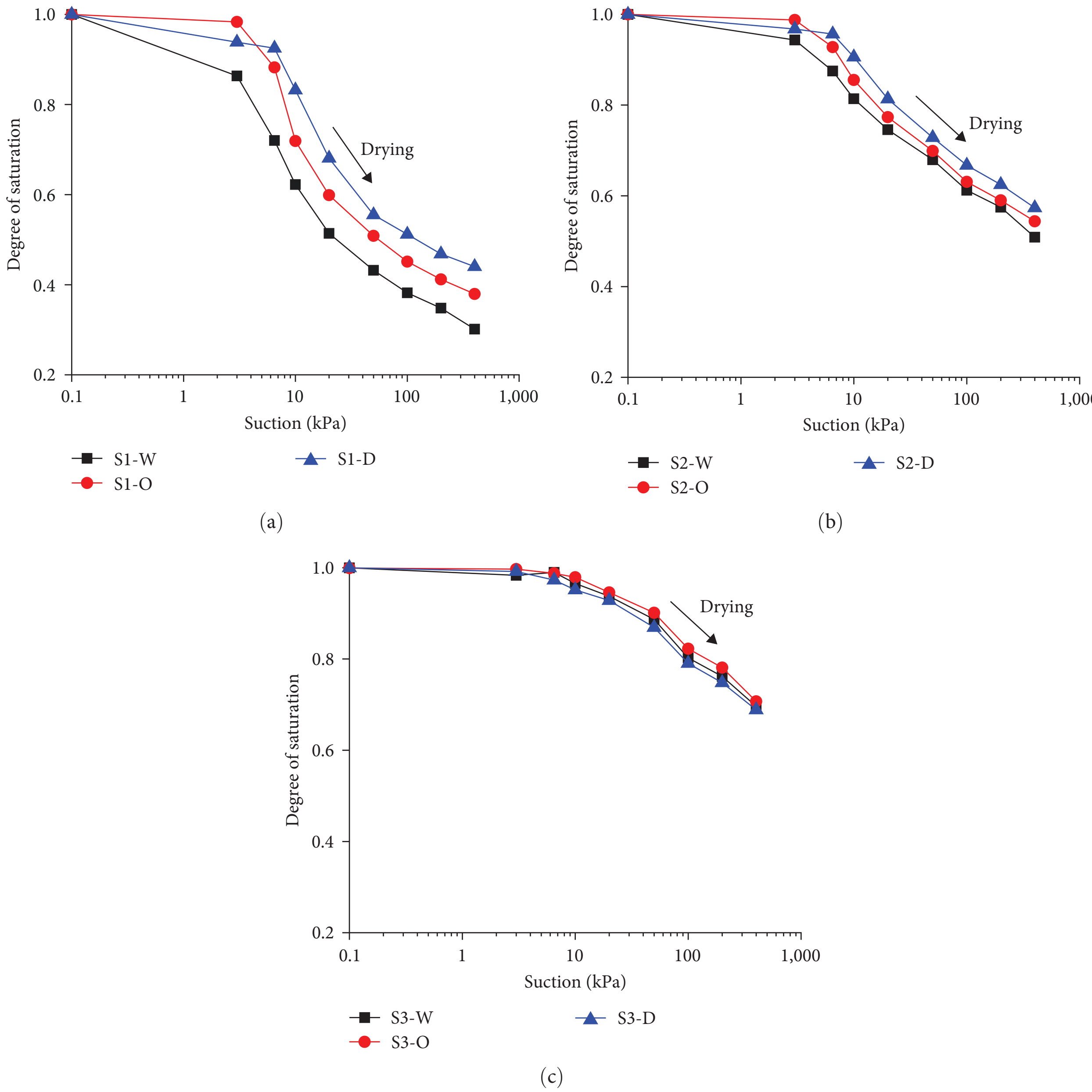

Figure 5: Water retention curves of specimens compacted at different water contents: (a) $p_{\mathrm{d}} = 1.3\ \mathrm{g/cm^3}$; (b) $p_{\mathrm{d}} = 1.53\ \mathrm{g/cm^3}$; (c) $p_{\mathrm{d}} = 1.73\ \mathrm{g/cm^3}$.

excessive water. These clods are relatively well preserved under lower compaction efforts (i.e., compaction dry density: 1.30 g/cm^3). The differences in particle arrangement and pore structure of the specimens at different compaction water contents have significant effects on their hydromechanical properties, which will be discussed in detail in the following sections. In practical engineering, the loess should be avoided to compacted at the wet side of optimum water content because of the formation of clods and large pores, as shown in Figure 4(c). The former increases the compressibility of compacted loess, while the latter promotes preferential flow under rainfall events. Both large compressibility and preferential flow are adverse to the settlement and stability control of infrastructure constructed with compacted loess.

5.2. Water Retention Behavior. Figure 5 shows the WRCs of loess along the drying path at different compaction water contents and compacted dry densities. For all specimens, the degree of saturation exhibits highly nonlinear relationships with respect to suction. The compaction water content affects the WRCs with various extents at different compaction dry densities. Furthermore, by comparing Figure 5(a)–5(c), the effects of compaction water content on WRCs almost diminish with increasing the compaction dry density from 1.30 to 1.73 g/cm^3. Previous studies identified three key quantitative parameters for WRCs: AEV, desorption rate, and residual water content [31]. The AEV is the suction in which air first enters the soil pores, while the desorption rate represents the drainage rate. The residual water content is the water

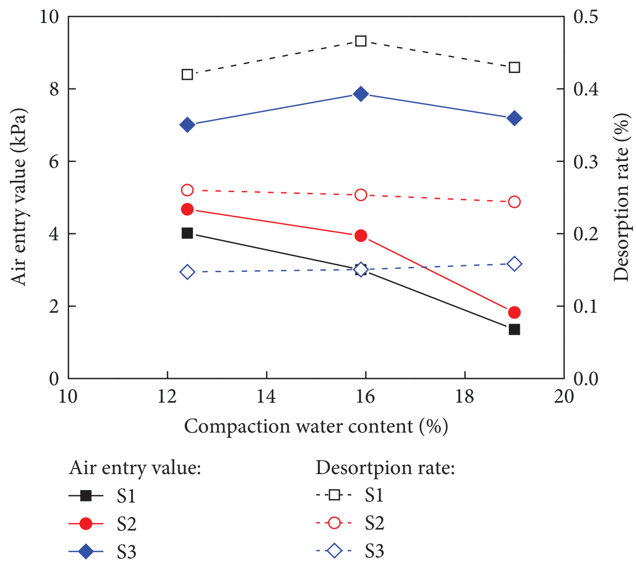

Figure 6: Air entry value and desorption rate of specimens compacted at different water contents.

content at the state where the water phase within the soil is discontinuous and isolated within thin films of water surrounding the soil and air [32].

Figure 6 shows the AEV and desorption rate of measured WRCs at different compaction dry densities and compaction water contents. At lower compaction dry densities (i.e., 1.3 and 1.53 g/cm^3), the AEV decreases by 64% with increasing the compaction water content from 12.4% to 19.0%. This is mainly due to the formation of large pores in the specimens at higher compaction water contents, as evidenced by the microstructure analysis (see Figure 4(c)). At a higher dry density, i.e., 1.76 g/cm^3), the influence of compaction water content on the AEV is insignificant (i.e., variation <1.5 kPa). This could be due to the larger compaction effort that breaks large pores between clods, resulting in a similar pore structure for the specimens at different compaction water contents [33, 34]. At a given compaction water content, the AEV increases with an increase in compaction dry density, which is consistent with previous studies [14–16]. On the other hand, the compaction water content has minor effects on the desorption rate at a given compaction dry density. This demonstrates that the desorption rate is primarily related to the void ratio and is independent of the pore structure. At a given compaction water content, the desorption rate decreases with an increase in compaction dry density.

5.3. Compression Behavior. Figure 7 shows the compression curves and variations in the suction of the specimens at different compaction and testing water contents. Comparisons of Figures 7(a), 7(c), and 7(e) show that the influence of compaction water content on the compression curve decreases with increasing the testing water content. In addition, the suction first remains almost constant at low vertical stresses and decreases with further increasing the vertical stress. Overall, higher compaction water contents allow the specimens to maintain larger suctions during the compaction. Based on Casagrande's [35] method, the yield stresses determined from the compression curves are presented in Figure 8. At a given testing water content of 14.7% (W1), 17.4% (W2), and 39.7% (W3), the yield stress decreases by 50.5%, 49.6%, and 18.5%, respectively, with the compaction water content increasing from 12.4% to 19.0%. These results demonstrate that the influence of compaction water content on the compression behavior of loess is more pronounced at lower testing water contents. This could be attributed to the coupling effects between the soil structure and suction, resulting in a stronger soil skeleton for specimens compacted at the dry side of optimum water content and at lower testing water contents. In addition, at a given compaction water content, the yield stress decreases with an increase in the testing water content. This can be explained by the suction-induced skeleton hardening effects [10, 16, 36, 37]. In addition, noted that the measured suctions at given water contents are different between water retention and compression tests. This is because the water retention tests are carried along a drying path, while the suctions measured in the compression tests follow a wetting path. Based on a previous study [38], there is a pronounced hysteresis in WRCs between drying and wetting paths.

5.4. Collapse Behavior. Figure 9 shows the collapse curves and suction variations of the specimens at different compaction water contents and a testing water content of 14.7%. In addition, the compression curves and suction variations of the specimens at testing water contents of 14.7% and 39.7% are also presented as references. The results indicate that the deformation and suction variation before and after soaking exhibit good agreement with the results obtained for the specimens at testing water contents of 14.7% and 39.7%, respectively. This is consistent with previous studies showing that a good consistency was observed between the single- and double-line methods for quantifying the loess collapse [19]. In addition, the good agreement demonstrates the reliability of the experimental results in this study. Based on the ASTM D5333-03 [39], the collapse index is defined as follows:

$$I_c = \frac{\Delta e}{1 + e_0}, \tag{1}$$

where Δe represents the variation in the void ratio of the specimen before and after wetting, and e_0 represents the initial void ratio. Based on Equation (1), the collapse indexes were calculated for the specimens at different compaction water contents, as shown in Figure 10. As the compaction water content increases from 12.4% to 19.0%, the collapse index decreases by 43.5%. This is primarily due to the fact that higher compaction water contents result in greater compression deformation under mechanical loading, thereby forming a stiffer soil skeleton. Consequently, the subsequent soaking-induced collapse is relatively smaller.

6. Summary and Conclusion

Based on laboratory tests, the influence of compaction water content on the water retention, compression, and collapse behavior of loess was investigated. Microscopic analysis was

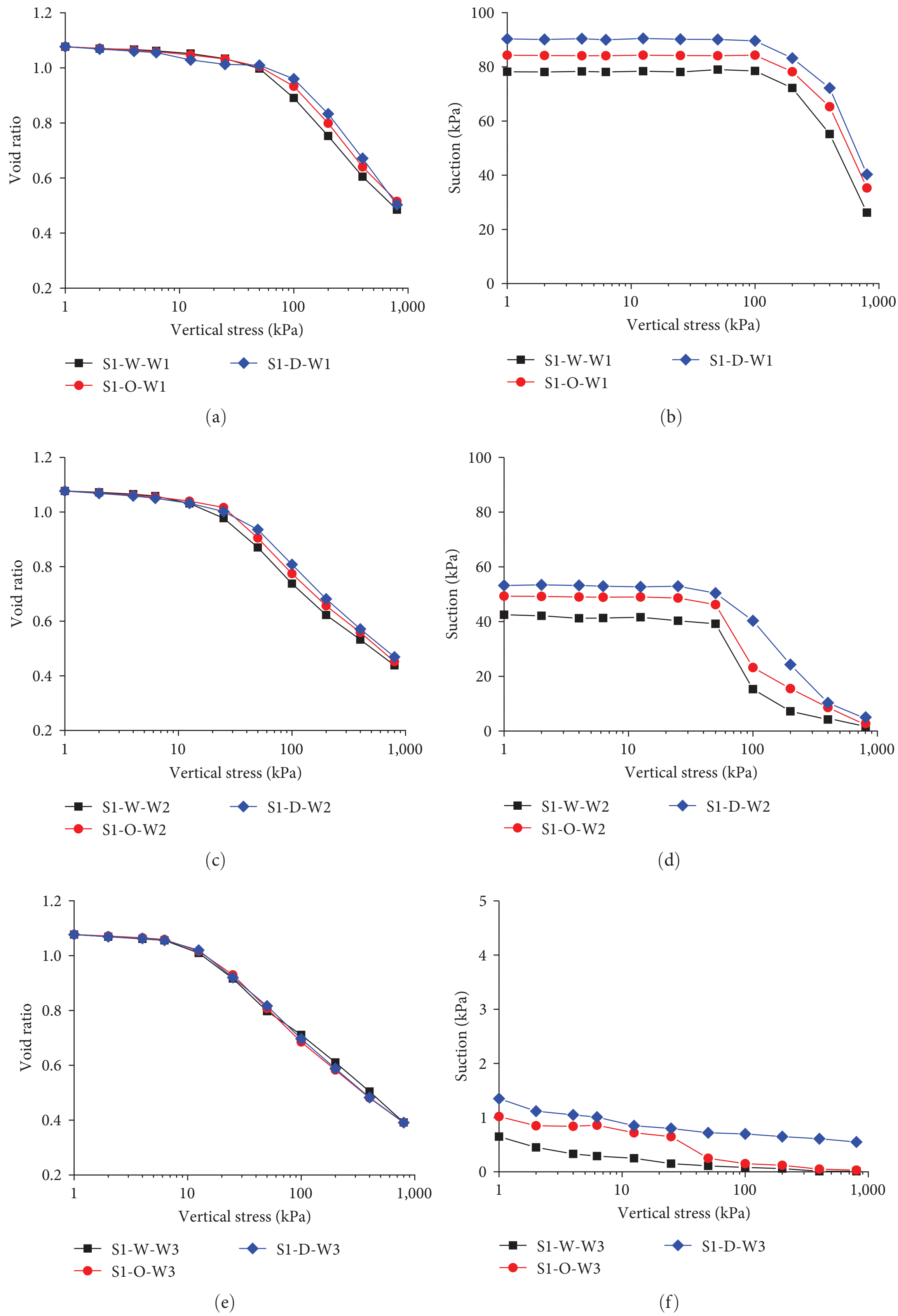

FIGURE 7: Compression behavior of specimens compacted at different water contents: (a) compression curve, S1-W1; (b) suction variation, S1-W1; (c) compression curve, S1-W2; (d) suction variation, S1-W2; (e) compression curve, S1-W3; (f) suction variation, S1-W3.

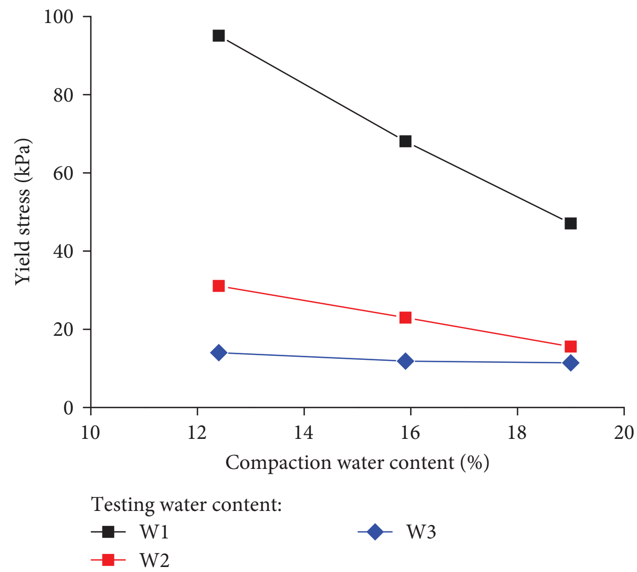

Figure 8: Yield stresses of specimens compacted at different water contents.

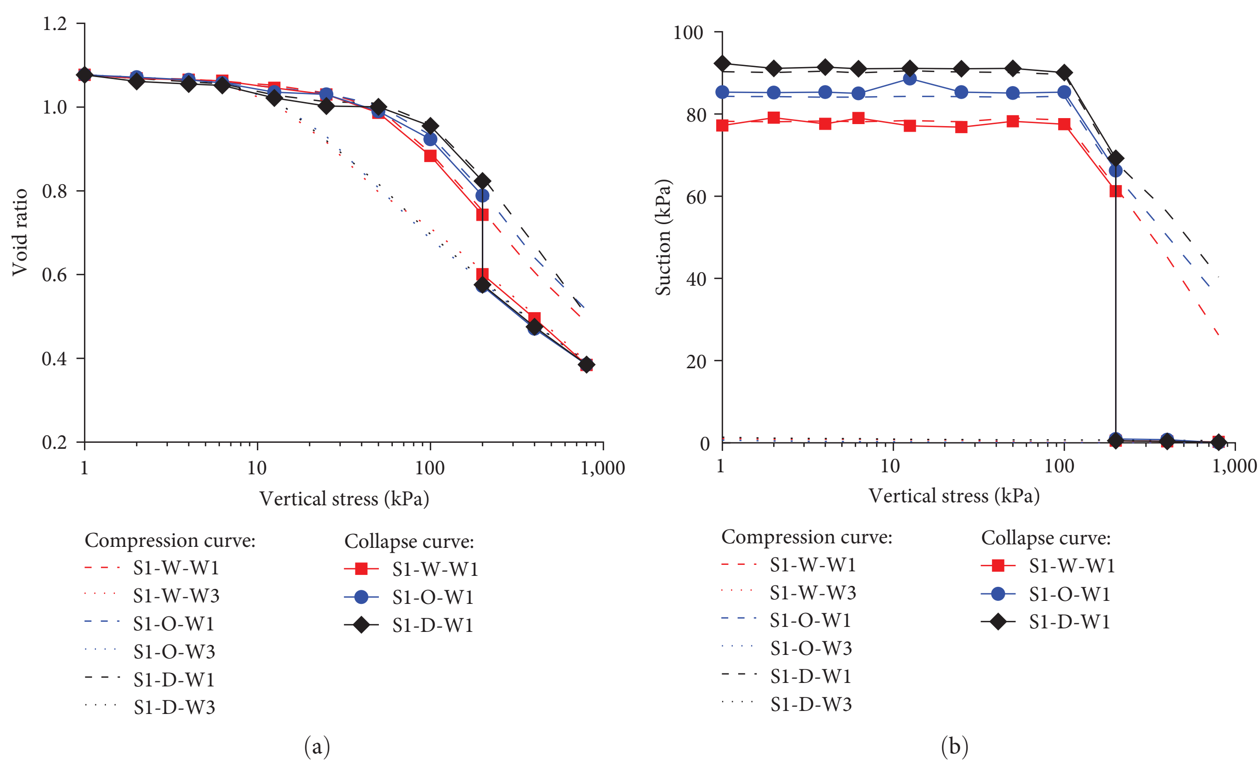

Figure 9: Collapse behavior of specimens compacted at different water contents: (a) collapse curve; (b) suction variation.

also carried out using a microscope to examine the microstructural differences of the compacted loess under different compaction water contents and provide insights into the interpretation of the test results. The main conclusions obtained in this study are as follows:

(1) As the compaction water content increases, the aggregate and pore sizes within the compacted loess increase. This is mainly due to the interaction between loess particles and water, resulting in the formation of large clods.

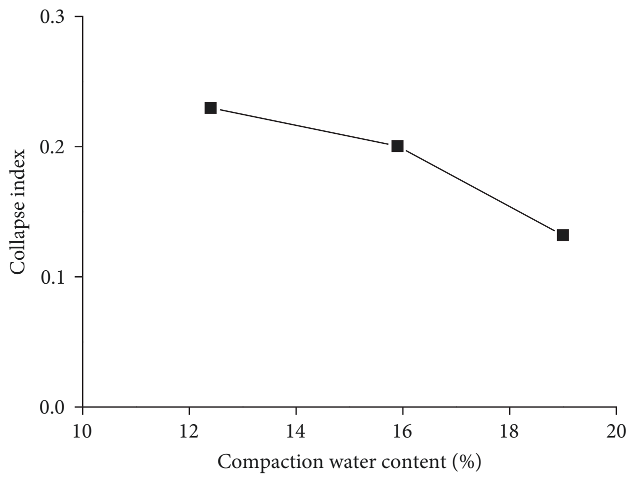

Figure 10: Collapse index of specimens compacted at different water content.

(2) The AEV decreases with an increase in compaction water content at a given compaction dry density, which is more pronounced at low compaction densities. In addition, the influence of compaction water content on the desorption rate is insignificant.

(3) The yield stress of compacted loess decreases with an increase in compaction water content, which is more pronounced at low testing water contents. This is mainly due to the formation of clods with low stiffness at higher compaction water contents, making the soil skeleton more susceptible to compression. In addition, the specimens at a compaction dry density of 1.3 g/cm^3 show smaller collapse indexes at higher compaction water contents. This is because the specimen has a larger deformation during the compression stage, resulting in a stiff skeleton during the subsequent soaking. The obtained results in this study are expected to provide scientific guidance for the usage of compacted loess as a construction material in practical engineering.

Data Availability

The data are available from the corresponding author upon reasonable request.

Conflicts of Interest

The authors declare that they have no conflicts of interest.

Acknowledgments

The authors acknowledge the National Science Foundation of China (52279109).

References

[1] L.-T. Zhan, Q.-W. Qiu, W.-J. Xu, and Y.-M. Chen, "Field measurement of gas permeability of compacted loess used as an earthen final cover for a municipal solid waste landfill," *Journal of Zhejiang University-Science A*, vol. 17, pp. 541–552, 2016.

[2] C. Zhu and N. Li, "Ranking of influence factors and control technologies for the post-construction settlement of loess high-filling embankments," *Computers and Geotechnics*, vol. 118, Article ID 103320, 2020.

[3] J. W. Zhang, Q. Y. Mu, A. Garg, F. L. Liu, and J. Cao, "Shear behavior of unsaturated intact and compacted loess: a comparison study," *Environmental Earth Sciences*, vol. 79, no. 3, pp. 1–14, 2020.

[4] K. Liu, K. Yuan, and B. Shi, "Study on prediction method for postconstruction settlement of Loess Fill Foundation in Northern Shaanxi, China," *Advances in Civil Engineering*, vol. 2020, Article ID 5703420, 11 pages, 2020.

[5] J. Li, S. Zhao, X. Wang et al., "Experimental study on consolidation characteristics of compacted loess," *Advances in Civil Engineering*, vol. 2021, Article ID 6687858, 12 pages, 2021.

[6] Y.-H. Liang, W.-H. Shui, and S.-F. Lu, "Field practice and ground settlement behaviors of a land creation case in loess area of China," *Bulletin of Engineering Geology and the Environment*, vol. 81, Article ID 462, 2022.

[7] C. Zhu, S. Peng, Z. Li, J. Xu, G. Deng, and S. Wang, "Evaluation on wetting effect of loess high-fill embankment under rainfall and groundwater uplift," *Transportation Geotechnics*, vol. 38, Article ID 100916, 2023.

[8] P. Delage, M. Audiguier, Y.-J. Cui, and M. D. Howat, "Microstructure of a compacted silt," *Canadian Geotechnical Journal*, vol. 33, no. 1, pp. 150–158, 1996.

[9] Q. Cheng, C. Zhou, C. W. W. Ng, and C. Tang, "Thermal effects on water retention behaviour of unsaturated collapsible loess," *Journal of Soils and Sediments*, vol. 20, no. 2, pp. 756–762, 2020.

[10] Q. Y. Mu, C. Zhou, and C. W. W. Ng, "Compression and wetting induced volumetric behavior of loess: macro- and micro-investigations," *Transportation Geotechnics*, vol. 23, Article ID 100345, 2020.

[11] Y. Yao, J. Ni, and J. Li, "Stress-dependent water retention of granite residual soil and its implications for ground settlement," *Computers and Geotechnics*, vol. 129, Article ID 103835, 2021.

[12] J. J. Ni, A. K. Leung, and C. W. W. Ng, "Modelling effects of root growth and decay on soil water retention and permeability," *Canadian Geotechnical Journal*, vol. 56, no. 7, pp. 1049–1055, 2019.

[13] J. Ni, J. Gu, and X. Zhao, "A hypoplastic model for unsaturated sand accounting for drying and wetting cycles," *Computers and Geotechnics*, vol. 165, Article ID 105879, 2024.

[14] F. Y. Liu, Z. Zhang, D. Zhou, X. G. Zhao, and L. Zhu, "Effects of initial density and drying–wetting cycle on soil water characteristic curve of unsaturated loess," *Rock and Soil Mechanics*, vol. 32, no. Supplement 2, pp. 132–136, 2011.

[15] T. Y. Zhao and J. F. Wang, "Soil-water characteristic curve for unsaturated loess soil considering density and wetting–drying cycle effects," *Journal of Central South University*, vol. 43, no. 6, pp. 2445–2453, (in Chinese), 2012.

[16] C. W. W. Ng, H. Sadeghi, S. K. B. Hossen, C. F. Chiu, E. E. Alonso, and S. Baghbanrezvan, "Water retention and volumetric characteristics of intact and re-compacted loess," *Canadian Geotechnical Journal*, vol. 53, no. 8, pp. 1258–1269, 2016.

[17] Q. Y. Mu, H. Dong, H. J. Liao, Y. J. Dang, and C. Zhou, "Water-retention curves of loess under wetting–drying cycles," *Géotechnique Letters*, vol. 10, no. 2, pp. 135–140, 2020.

[18] Q. Mu, L. Meng, Z. Lu, and L. Zhang, "Hydro-mechanical behavior of unsaturated intact Paleosol and intact loess," *Engineering Geology*, vol. 323, Article ID 107245, 2023.

[19] Q. Y. Mu, Y. J. Dang, Q. Dong, H. J. Liao, and H. Dong, "Water-retention characteristics and collapsibity behaviors: comparison between intact and compacted loesses," *Chinese Journal of Geotechnical Engineering*, vol. 41, no. 8, pp. 1496–1504, (in Chinese), 2019.

[20] J. J. Wang, Y. Z. Hao, and T. H. Wang, "Experimental study of structural characteristics of unsaturated compacted loess," *Rock and Soil Mechanics*, vol. 40, no. 4, pp. 1351–1357, (in Chinese), 2019.

[21] X. F. Huang, Y. Kong, X. D. Li, L. Ma, and B. S. Yang, "Study and application of deformation characteristics of compacted loess," *Rock and Soil Mechanics*, vol. 35, no. 2, pp. 37–44, (in Chinese), 2014.

[22] C. L. Chen, X. Jiang, J. Yang, J. Zhang, and J. Xue, "Influence of soil structure on confined compression behavior of compacted loess," *Chinese Journal of Rock Mechanics and Engineering*, vol. 33, no. 9, pp. 1939–1944, (in Chinese), 2014.

[23] Y. S. Yang, J. Li, Y. C. Xing, and J. M. Zhao, "Experimental study on moistening deformation characteristics of compacted loess and their influencing factors," *Chinese Journal of Geotechnical Engineering*, vol. 39, no. 4, pp. 626–635, (in Chinese), 2017.

[24] J. Wang, S. J. Shao, and P. Chen, "Experimental study of soil water properties, compression yield and collapse deformation of unsaturated remolded loess," *Rock and Soil Mechanics*, vol. 38, no. Supplement 2, pp. 217–222, (in Chinese), 2017.

[25] R. Chen, J. Liu, J. H. Li, and C. W. W. Ng, "An integrated high-capacity tensiometer for measuring water retention curves continuously," *Soil Science Society of America Journal*, vol. 79, no. 3, pp. 943–947, 2015.

[26] GB/T 50145, "Engineering classification standard for soil," Beijing, China, China Planning Press: Beijing, China (in Chinese), 2007.

[27] ASTM, "Standard test methods for liquid limit, plastic limit, and plasticity index of 279 soils," ASTM International, ASTM D4318-10, 2010.

[28] ASTM, "Standard test methods for laboratory compaction characteristics of soil using standard effort," ASTM International, ASTM D698-12, 2021.

[29] P. Li, Z. Pan, T. Xiao, and J. Wang, "Effects of molding water content and compaction degree on the microstructure and permeability of compacted loess," *Acta Geotechnica*, vol. 18, no. 2, pp. 921–936, 2023.

[30] L. Deng, W. Fan, S. Liu, Y. Chang, Y. Dai, and Y. Li, "Quantitative research and characterization of the loess microstructure in the Bai Lu Tableland, Shaanxi Province, China," *Advances in Civil Engineering*, vol. 2020, Article ID 3681382, 14 pages, 2020.

[31] D. G. Fredlund and A. Xing, "Equations for the soil–water characteristic curve," *Canadian Geotechnical Journal*, vol. 31, no. 4, pp. 521–532, 1994.

[32] S. K. Vanapalli, D. G. Fredlund, D. E. Pufahl, and A. W. Clifton, "Model for the prediction of shear strength with respect to soil suction," *Canadian Geotechnical Journal*, vol. 33, no. 3, pp. 379–392, 1996.

[33] P. Xu, H. Qian, S. Li, W. Li, J. Chen, and Y. Liu, "Geochemical evidence of fluoride behavior in loess and its influence on seepage characteristics: an experimental study," *Science of The Total Environment*, vol. 882, Article ID 163564, 2023.

[34] P. Xu, H. Qian, W. Li, W. Ren, F. Yang, and L. Wang, "New insights into the seepage behavior of heavy metal-contaminated loess and its underlying geochemical mechanism," *Journal of Hydrology*, vol. 620, Article ID 129476, 2023.

[35] A. Casagrande, "The determination of pre-consolidation load and its practical significance," in *Proceedings of the International Conference on Soil Mechanics and Foundation Engineering*, pp. 60–64, Harvard University, Cambridge, MA, 1936.

[36] E. E. Alonso, A. Gens, and A. Josa, "A constitutive model for partially saturated soils," *Géotechnique*, vol. 40, no. 3, pp. 405–430, 1990.

[37] Q. Wang, X. Yan, Y. Dong, W. Su, Y. Meng, and W. Sun, "Effect of Beishan groundwater salinity on the self-sealing performance of compacted GMZ bentonite," *Environmental Earth Sciences*, vol. 82, Article ID 391, 2023.

[38] Q. Y. Mu, L. L. Meng, and C. Zhou, "Stress-dependent water retention behaviour of two intact aeolian soils with multimodal pore size distributions," *Engineering Geology*, vol. 323, Article ID 107233, 2023.

[39] ASTM D5333-03, "Standard test method for measurement of collapse potential of soils," Annual Book of ASTM Standards, ASTM International, West Conshohocken, PA, 2003.